Performance Comparison Update: GLAST18/35

S. Digel (USRA/GSFC), 6 Oct 2000

This document extends the comparison of GLAST25 and GLAST35 (Digel & Norris, 12 May 2000) to include a 'hybrid' version, called GLAST18/35 here.

Definitions:

GLAST25: AO configuration, 12 layers with 2.5% RL then 4 layers with 25% RL converter foils

GLAST35: 16 layers with 3.5% RL foils ("GLAST Classic")

GLAST18/35: 12 layers with 3.5% RL foils then 4 layers with 18% RL converter foils

All configuations have two layers at the bottom with no converters

Point-spread Function (GLAST25 & GLAST35):

Derived from runs of Glastsim for a grid of energies and inclination angles

After all background & PSF cuts were applied, histograms of angular errors were fit with the sum of two Gaussians (3 free parameters)

This is an improvement of the definition of the PSF relative to the simulations for the AO response, for which only two parameters could be fit (a fixed relative weight of the narrow and broad Gaussians was adopted)

Point-spread Function (GLAST18/35):

Approximated. For the front section, the PSF of GLAST35 was used. For the back section, the PSF of the back section of GLAST25 was used

Effective Area:

GLAST25: The same effective area arrays for the front and back sections as were used for the simulations in the AO response. Peak effective area is 12,100 cm^2 (5400 cm^2 front/ 6700 cm^2 back).

GLAST35: Effective area was scaled from the effective area of the front section of GLAST25, taking into account the difference in overall thickness (in RL). This is an approximation. Peak effective area is 8300 cm^2.

GLAST18/35: Also approximated. Effective area of the front section was scaled from the front section of GLAST25, increasing the converter thickness from 2.5% to 3.5%. For the back section, the effective area was scaled from the back section of GLAST25 to account for the decreased converter thickness (18% vs. 25%) and the increased attenuation of the front section. Peak effective area is 11,000 cm^2 (6400 cm^2 front/4600 cm^2 back)

Figure of Merit	Source Flux (cm^{-2} s^{-1})	GLAST25	GLAST35	GLAST35/25
1 Flux Limit				√
High Latitude (cm^{-2} s^{-1})		3.5E-09	3.8E-09	3.4E-09
Low Latitude (cm^{-2} s^{-1})		1.0E-08	1.0E-08	1.0E-08
Diam. 95% Confidence Region			√	
High Latitude	5E-08	0.035°	0.030°	0.031
	2E-08	0.068	0.057	0.063
	1E-08	0.12	0.10	0.10
Low Latitude	5E-08	0.037°	0.033	0.03
	2E-08	0.098	0.094	
	1E-08	0.20	0.16	
2 Min. Separation			√	
Two sources of the indicated flux at high latitude	1E-07	0.09°	0.07°	
	5E-08	0.11	0.09	
	2E-08	0.17	0.15	0.14
	1E-08	0.24	0.22	0.22
3 Precision of Spectral Meas. for a Flaring Source (>10 GeV)		√		
One-week observation of a source with the indicated flux and $\alpha = -2$.	1E-05	±0.12	±0.16	
	5E-06	±0.17	±0.23	
	2E-06	±0.27	±0.34	
	1E-06	±0.44	±0.54	
4 Precision of Spectral Meas. for a Faint Source Near a Bright One				
<100 MeV (see Fig. 1)	5E-08		√	
>3 GeV	5E-08	√		
(bright src. is 10× flux, 0.5° away)				
5 Resolving Small Extended Source		(√)	√	
Min. ang. diam. for resolving	2E-08	0.45°	0.40°	0.42
Max. ang. diam. for detecting	2E-08	5.0	4.2	
6 Smallest Timescale		√		
Doubling from initial flux to the indicated flux	2E-06	19 min	22 min	

Notes:

All FoM: Significances for source detection and source resolution are 5 σ. Unless otherwise stated, all values apply to a one-year sky survey. Point sources are assumed to have photon spectral indicies -2 and fluxes are quoted for energies >100 MeV. The diffuse background emission is assumed to be isotropic, with photon spectral index -2. 'High latitude' means isotropic intensity 2.0×10^{-5} cm^{-2} s^{-1} sr^{-1} (representative for $|b| \sim 60°$) and 'Low latitude' means isotropic intensity 23.3×10^{-5} cm^{-2} s^{-1} sr^{-1} (both >100 MeV), the average intensity for $|b| < 5°$.

FoM 2: Minimum angular separation (deg) between two sources of equal flux (specified for $E > 100$ MeV) observed against a high-latitude background. The angles quoted are for 5 σ distinction between one and two sources.

FoM 3: These are the 1 σ uncertainties in the spectral index for energies >10 GeV for a flaring source observed for one week against a high-latitude background. See Figure 2. The brightest flares seen by EGRET are $\sim 2 \times 10^{-5}$ cm^{-2} s^{-1} (>100 MeV) for at least several days.

FoM 4: For Figure 1, a source of the indicated flux was simulated 0.5° from a source with 10 times the flux, and the same spectrum. The figure shows the ±1 σ uncertainty of the measured flux of the fainter source for several energy ranges. Below 100 MeV, the GLAST25 could not measure the flux separately from that of the brighter source.

FoM 5: The first entry is the minimum angular size (diameter in deg) for a small extended source of specified flux to be distinguished from a point source when observed against a high-latitude background. The second entry is the maximum angular size for the source to be detected at all. For convenience in simulation, the source is assumed to be square.

FoM 6: Indicated are the times required for a 5-σ detection of a source of the indicated flux for a pointed observation with the source at the center of the field of view.

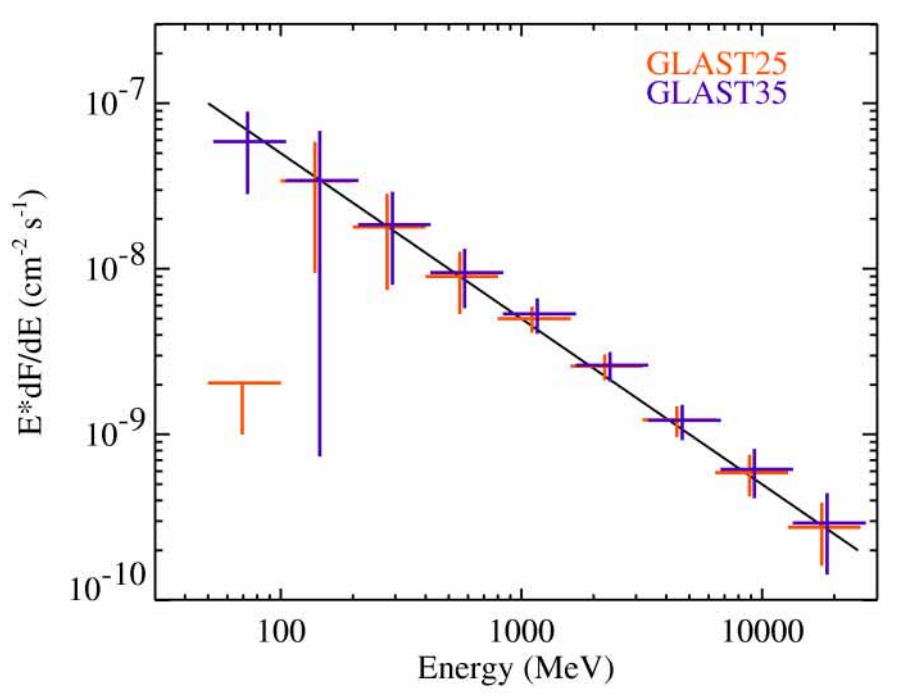

Figure 1. Comparison of precision of spectral measurement for source of flux 5E-08 cm^{-2} s^{-1} (approximately EGRET's detection limit). See Figure of Merit 4.

Figure 2. Uncertainties of measured spectral index in a one-week observation

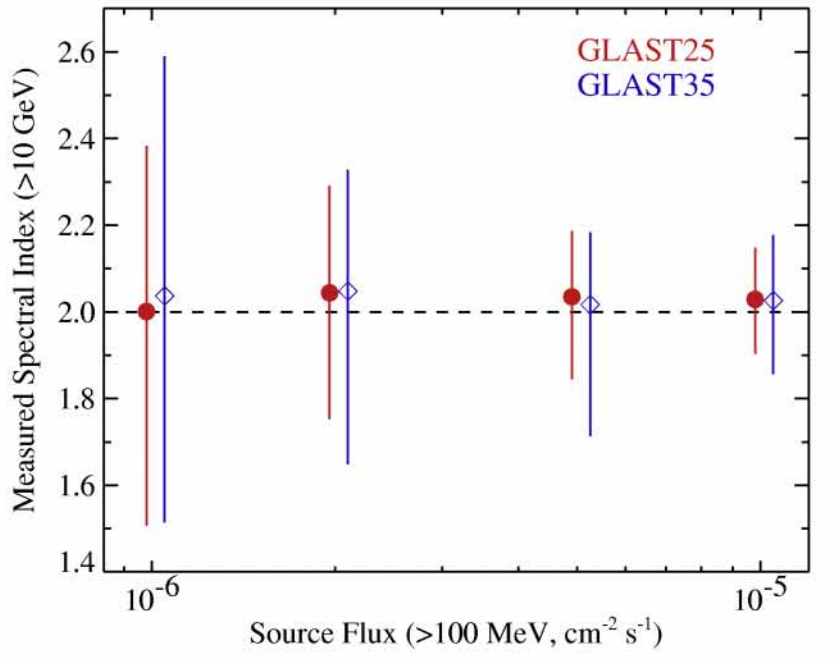

during the sky survey. See FoM 3.